

Fever and mobility data indicate social distancing has reduced incidence of communicable disease in the United States

Parker Liautaud ^{*1}, Peter Huybers¹, and Mauricio Santillana^{2,3}

¹Department of Earth and Planetary Sciences, Harvard University, Cambridge, MA, USA

²Computational Health Informatics Program, Boston Childrens Hospital, Boston, MA, USA

³Department of Pediatrics, Harvard Medical School, Boston, MA, USA

April 22, 2020

Abstract

In March of 2020, many U.S. state governments encouraged or mandated restrictions on social interactions to slow the spread of COVID-19, the disease caused by the novel coronavirus SARS-CoV-2 that has spread to nearly 180 countries. Estimating the effectiveness of these social-distancing strategies is challenging because surveillance of COVID-19 has been limited, with tests generally being prioritized for high-risk or hospitalized cases according to temporally and regionally varying criteria. Here we show that reductions in mobility across U.S. counties with at least 100 confirmed cases of COVID-19 led to reductions in fever incidences, as captured by smart thermometers, after a mean lag of 6.5 days (90% within 3–10 days) that is consistent with the incubation period of COVID-19. Furthermore, counties with larger decreases in mobility subsequently achieved greater reductions in fevers ($p < 0.01$), with the notable exception of New York City and its immediate vicinity. These results indicate that social distancing has reduced

*Corresponding author, e-mail: parker.liautaud@g.harvard.edu

the transmission of influenza like illnesses, including COVID 19, and support social distancing as an effective strategy for slowing the spread of COVID-19.

1 Introduction

A new betacoronavirus, SARS-CoV-2, was identified in the city of Wuhan in China's Hubei Province in December, 2019 [50]. Despite efforts to contain it, the disease caused by this virus, COVID-19, spread rapidly across Chinese provinces in January of 2020 and around the world in February and March. As of April 19, 2020, more than 2 million confirmed cases of COVID-19 have led to over 150,000 deaths [44], with the United States (U.S.) accounting for a plurality of both.

In the absence of an effective vaccine against the virus or a reliable treatment for COVID-19, the primary public health strategy for slowing transmission has been to encourage or mandate the minimization of all but essential face-to-face human interactions, known as social distancing. Such interventions seek to limit opportunities for transmission by reducing the number of individuals exposed by each newly infected individual. That is, social distancing is intended to decrease the reproductive number of COVID-19 [24, 26]. Implemented social distancing policies in the United States have included closing businesses, restricting large gatherings, and encouraging or requiring residents to stay at home unless undertaking essential tasks [11]. These strategies complement other non-pharmaceutical interventions such as contact tracing and isolation or quarantine of individuals suspected to be infected with COVID-19 [11, 13, 46].

Reliable metrics for the impact of social distancing measures on COVID-19 transmission would be useful for informing which are most effective and when and how they should be deployed. Studies of COVID-19 spread in China [5, 17, 20], Italy [35], and globally [13] have relied upon confirmed case statistics to evaluate the effectiveness of non-pharmaceutical interventions in slowing the spread of the disease. Confirmed COVID-19 case counts are difficult to interpret, however, owing to uncertainties associated with what fraction of cases are captured in test statistics [15, 43] and high false-negative rates associated with tests [52]. Furthermore, case

reports inevitably lag the onset of illness [48]. Other studies have used deaths from COVID-19, which are more likely to be recorded than infections, but these represent a small portion of the population and lag disease transmission by two or more weeks [53].

Numerous decentralized data sources informing the health and behavior of millions of individuals have become available over the last decade, motivating the development of new methodologies intended to track and ultimately limit the spread of diseases at the population level [37]. To estimate disease activity, these approaches have exploited near real-time data from internet search engines [12, 40, 51], clinicians search engines [39], news reports [1], crowd-sourced participatory disease surveillance systems [33, 42], Twitter micro-blogs [34], electronic health records [38, 47], Wikipedia traffic [10], wearable monitoring devices [36], satellite images [31], and smartphone-based digital thermometers [27]. These new sources of data suggest the potential to achieve near real-time monitoring that is sufficiently complete to infer representative population-wide characteristics and disease trends. In exchange, control over sampling protocols and participant behavior is typically lost, risking the introduction of systematic bias and requiring care in interpretation.

In this study we use daily estimates of travel distances from cell-phone data and the incidences of fever from a network of smart thermometers across the U.S. to investigate whether the adoption of social distancing practices has slowed the transmission of communicable fever-causing illnesses, including COVID-19. It should be emphasized that the use of novel data to inquire into the dynamics of a novel disease in response to unprecedented changes in social behavior is liable to lead to bias and misinterpretation. By way of example, attempts to predict seasonal influenza from Google search patterns appeared skillful over multiple seasons, but failed to forecast the 2009 H1N1 (“Swine Flu”) pandemic and overestimated the spread of the 2013 seasonal influenza in the United States by a factor of nearly two [2, 6, 22, 40]. Our aim, therefore, is not to establish the response of COVID-19 to doses of social distancing, but to investigate whether two decentralized data sets may be leveraged to identify patterns consistent with the dynamics of COVID-19.

2 Data and methods

Aggregated mobility data are provided by the location analytics company Cuebiq through its Data for Good program. Cuebiq collects first-party location information from smartphone users who opted in to anonymously provide their data through a GDPR-compliant framework. Location data are aggregated into an index, M , defined as the base-10 logarithm of median distance traveled per user on each day. For users traversing county borders, their movement is recorded as belonging to the county in which they spend the most time on a given day. In order to better focus our analysis on COVID-19, only counties having at least 100 confirmed cases of COVID-19 as of April 10 are included, giving a total of 368 counties.

We quantify decreases in mobility between March 5 and April 15 using the range in mobility divided by its maximum value, $\delta M = 100 \times (M_{\max} - M_{\min})/M_{\max}$, where the factor of 100 corresponds to reporting δM as a percentage. M is first smoothed with a 7-day moving average to eliminate a weekly cycle associated with reduced commuting during weekends. Although, in principle, δM could be ambiguous with respect to increasing or decreasing values of mobility, in practice, all smoothed mobility data show a clear structure of nearly stable values followed by a marked decline. If δM was computed between January 1 and March 4 it would average only 10%, whereas in our selected March 5 to April 15 window δM averages 54%, with 95% of counties having values between 21% and 96%. These major decreases in mobility coincide with the voluntary and enforced restrictions on movement and business activity introduced in mid-March in many U.S. states [11].

Fever incidence data comes from a network of smart-phone connected personal thermometers managed by Kinsa, Inc. [4]. Kinsa began monitoring fevers in 2013, and the results of their distributed thermometer network correlate closely with reported ILI cases from the U.S. Centers for Disease Control (CDC) across regions and age groups in previous years [27]. Aggregated and anonymized fever incidence is reported daily at the level of counties for the contiguous 48 states. Daily fever rates in a given county are calculated as the number of fevers reported divided by the number of unique users within the last year, where a fever is defined as a persistent temperature

above 37.7°C . Despite having more than a million users across the U.S., Kinsa finds it necessary to drop estimates in certain counties whose user base is too small, based upon comparison of their fever tracking against CDC ILI estimates [3], and instead reports values interpolated from neighboring counties. At the time of writing, we do not know which county estimates are from thermometer data versus being interpolated, and we instead attempt to control for this effect through spatial averaging. Finally, a linear calibration is applied to the fraction of users experiencing fevers that is determined at the national level in comparison to CDC ILI estimates between August 2016 through August 2019.

For purposes of analysing whether reductions in mobility are associated with reductions in fevers, we compute a percentage decrease in fevers from Kinsa data similar to that used for mobility, $\delta F = 100 \times (F_1 - F_2)/F_1$. In this case, F_1 and F_2 represent the average fever incidence, respectively, over the ten days before a drop in mobility and from ten to twenty days afterwards. The ten-day interval between the end of F_1 and beginning of F_2 is introduced to account for the time required for a reduction in transmission to manifest as a change in fevers. The drop in mobility is defined as occurring on the day at which the smoothed mobility signal decreases to halfway between its maximum and minimum values.

Limitations. There are several sources of uncertainty in assessing the degree to which changes in mobility are responsible for changes in fever incidence, foremost that mobility and fever incidence are proxies for the actual variables of interest. The distance traveled by smartphone users does not, for example, account for the fact that walking on a crowded street involves greater likelihood of close human contact than does driving on an open highway. Similarly, fever data do not distinguish between cases arising from COVID-19, influenza, or any other illness that causes fever. Furthermore, the contribution of COVID-19 is difficult to estimate using fever statistics from previous years because mobility changes are expected to influence transmission of most febrile respiratory infections. The signal of COVID-19 in fever data is also expected to under-represent its actual spread in the population because only approximately 40% of COVID-19 cases manifest with fevers [30]. An additional source of uncertainty arises from seasonality.

ILI is strongly seasonal, decreasing through March and April in most years regardless of changes in mobility [28], and COVID-19 dynamics may also be found to be seasonal, albeit to an unknown extent [29]. These factors inform our decision to focus on county-level patterns in the rates of fractional fever reduction as opposed to the absolute magnitude of fever declines.

3 Results

Our analysis is divided into three sections. We first examine the relative timing of reductions in mobility and fevers (Figure 1), and next the magnitude of reductions in fevers relative to changes in mobility (Figures 2 and 3). Whereas most counties apparently follow a relationship whereby greater mobility reductions lead to greater reduction in fevers (Figure 3a), counties in the vicinity of New York City follow a distinct pattern (Figure 3b) that we discuss in a final section.

3.1 Timing of reductions in mobility and fevers

We first inquire as to the plausibility of a causal relationship between changes in fevers and mobility. Specifically, a mobility-induced change in fever incidence should lag the change of mobility by a time equal to or longer than the incubation period of COVID-19. We estimate the lead or lag between reductions of mobility and reduction in fevers as the time shift that minimizes their mean-squared difference. The lead-lag analysis is computed using time-series of F and M as defined in the methods section, from March 5th, selected for being prior to systematic changes in mobility, to April 15, representing the most current data at the time of our analysis. On average, changes in fevers are found to lag changes in mobility by 6.5 days, with 95% of the 368 counties included in the analysis having lags between 3 and 10 days (Figures 1 and S1). This lag agrees with independent estimates of the incubation period of COVID-19 as averaging 6 days and ranging between 2 and 14 days [19, 21, 23, 25]. Observed lags are also consistent with estimates for negative growth rates of COVID-19 cases occurring 8 to 12 days after nation-wide restriction in travel in China [18], once accounting for the fact that an

additional lag averaging 4.8 days arises between the onset of symptoms, such as fever, and the confirmation of a COVID-19 infection.

Despite consistency with COVID-19 epidemiology, a range of lagged responses to reductions in mobility are expected to be present within our analysis of fevers. Incubation times for various human-to-human communicable and fever-causing diseases range from as short as 1 to 2 days for influenza to several weeks or longer for other diseases [41]. Although not undertaken herein, more detailed analysis of the relative contributions of COVID-19, influenza, and other illnesses to the fever signal might permit for distinguishing the degree to which close agreement of the observed lag with the COVID-19 incubation period is indicative of COVID-19 prevalence or, instead, arises from a combination of diseases.

3.2 Magnitudes of reductions in mobility and fevers

We next consider whether the magnitude of mobility reductions are predictive of the magnitude of the subsequent fever reductions, examining the 368 counties that each have more than 100 confirmed COVID-19 cases. An overall decrease is anticipated solely on the basis of seasonal declines in ILI, but the average seasonally-attributable δF , as reported by Kinsa, is only expected to average 28%. In contrast, the observed decline in fevers in 2020 is more than double the expected value with an average δF of 79%. The anomalously large reduction in fevers is consistent with the twin effects of an excess of fevers increasing F_1 to 31% above its seasonally-expected value and social distancing subsequently reducing F_2 to 63% below its expected value.

Ordinary least-squares regression of δF against δM indicates a $0.81 \pm 0.28\%$ decline in fever incidence with each 10% reduction in mobility ($p < 0.01$, Figure 3a). Two potential concerns with such a simple regression are that the p -value is estimated assuming that counties are independent, and that noise in the predictor values causes regression dilution [9] that biases results toward a shallower slope. A second regression is, therefore, performed after spatially averaging mobility and fever reductions into 5° latitude by 5° longitude bins such that data from 368 counties are represented by 34 grid boxes that are expected to have greater independence

and less noise. Regression at this 5° by 5° scale gives a steeper slope indicating a $2.1 \pm 0.6\%$ reduction in fever incidence per 10% reduction in mobility ($p < 0.01$) that we consider to be more accurate (Figure S3).

It is useful to briefly review the patterns of mobility and fever reduction across the U.S. that underlie our regression results (Figure 2). The 24 counties in Washington and California with the largest decreases in mobility ($\delta M > 90\%$) experienced an average reduction in fever incidences of 90% (range of 85–93%). Estimated incidences in these counties all decreased to less than 0.7% of the population after mobility reduction, whereas they averaged 4.8% prior to the change in mobility. More moderate reductions in fever incidence are found in counties with smaller mobility reductions. Counties having δM less than 25%, for example, are all located in South Carolina, Florida, Tennessee, Alabama, Missouri, or Georgia, and are associated with an average reduction in fevers of 80% (range of 67–89%).

The fact that the y -intercept of our regression of δF onto δM is $72 \pm 4\%$, using the spatially-averaged data, indicates that there are factors acting to reduce fever incidence nationwide irrespective of changes in mobility. Such a relationship is expected, as noted, on the basis of the seasonality associated with influenza [28], although seasonality is only expected to account for approximately one-third of the intercept value. A greater-than-expected y -intercept may arise if COVID-19 also responds to seasonal changes in environmental conditions, although whether such a sensitivity exists is presently unclear [29]. Additional factors may include broad adoption of behaviors that limit disease transmission but may not influence travel distances – such as individuals remaining more dispersed in public, regularly disinfecting surfaces, and more frequently washing their hands – as well as an approximately 60% decline in U.S. air travel in March and April relative to 2019 [32].

The other major feature associated with the regression is a cluster of outliers that share the distinction of being near New York City (Figure 3a), and which are treated separately in the following subsection. Omitting counties within 500 km of New York City gives a higher county-level regression slope of a $1.6 \pm 0.13\%$ decrease in fevers for each 10% reduction in mobility

($p < 0.01$, Figure 3a). At the 5° by 5° degree grid level, again omitting counties within New York City’s sphere of influence, the slope is $2.0 \pm 0.4\%$ for each 10% reduction in mobility ($p < 0.01$; Figure S3). Thus, we find a significant regression relationship between mobility and fever reduction whose magnitude is consistent with the latter estimate of $2.0 \pm 0.4\%$ for plausible choices regarding averaging and omission of outliers.

3.3 New York City and neighboring counties

As of mid-April, New York City had the highest rate of confirmed COVID-19 infections of any region, accounting for over 30% of the nation’s confirmed cases. Changes in fevers in the five boroughs comprising New York City are, however, not explained by their changes in mobility (Figure 3). Although New York City has achieved amongst the highest levels of mobility reduction, with its five boroughs averaging a δM of 81% and Manhattan having a δM of 95%, the city’s fever reductions are amongst the smallest in the country with a δF of only 53%.

Fever reductions have been more successful further from New York City. A regression of δF against distance from Central Park in Manhattan for counties up to 500 km away indicates that δF increases by 7% per additional 100 km distance from Manhattan ($r = 0.87$, $p < 0.01$). Reductions in mobility, δM , are greatest in the immediate vicinity of New York City, resulting in a weak regional anti-correlation with δF ($r = -0.45$). County-level population density also weakly corresponds with δF such that higher population density is associated with less reduction in fever ($r = -0.38$), as expected [7]. Multiple linear regression using δM , population density, and distance from New York City to predict δF , however, indicates that only distance makes a statistically significant contribution. These results may expose the limitations of our using a single quantification of human mobility as a proxy for human-to-human contact in that it does not capture, for example, if individuals move from more highly infected regions elsewhere.

As has been found to be generally possible in hierarchical metapopulation models [49], we suggest that counties within 500 km of New York City continue to experience relatively high rates of fevers – despite substantially reducing their local mobility – because no strict travel

restrictions were imposed to protect them from the city’s high infection rates. In contrast with China’s restrictions on travel to and from Wuhan that appear to have dramatically reduced the city’s ability to seed new outbreaks elsewhere [5, 18], New York City opted instead to focus on local social-distancing efforts [11]. The outstanding question for this region then appears to be why rates of fever have remained relatively high in New York City despite its massive reduction in mobility, with possibilities including that the city is more densely populated than any other in the U.S. [7, 45] and that it may have experienced substantial community spread of COVID-19 prior to the implementation of social-distancing rules [14].

4 Further discussion and conclusion

In agreement with foregoing studies [5, 13, 18, 20], our results indicate that social distancing has limited the spread of COVID-19. Many U.S. counties with large reductions in mobility achieve near-zero fever incidences by early April, indicating that severe curtailment of mobility is effective in reducing disease transmission. Some counties in Midwestern states, however, achieve similar outcomes with more moderate mobility reductions, and New York City has only partially reduced fevers despite strong decreases in mobility. These counter-examples highlight that regional disparities in demographics, climate, or the delay before implementing mobility restrictions are also potentially of first-order importance for explaining and predicting the spread of COVID-19.

The corollary to social distancing being effective is the question of the optimal degree of mobility restriction for purposes of controlling the spread of COVID-19. Foregoing studies have generally drawn inferences from confirmed case statistics [5, 13, 18, 20], but these lag actual infections by up to several weeks and are subject to heterogeneous and potentially biased reporting, making it challenging to infer causality in case growth rates and possibly allowing outbreaks to spread through communities before a response can be mounted. Our combining cell-phone mobility insights with smart-thermometer fever data permits for more rapidly assessing the timing and rates of change in illness incidence. By leveraging existing data sources for

disease surveillance, approaches like the one we have employed may enable timely monitoring of the effectiveness of mobility restrictions and, thereby, support efforts to contain emerging outbreaks [8]. The importance of such capabilities is underscored by the possibility that COVID-19 outbreaks will recur seasonally and require prolonged or intermittent social distancing [16].

Acknowledgements

Cuebiq made their county-level mobility data available for this study, and Kinsa made their county-level smart thermometer data public. Comments by Col. Downing Lu (U.S. Army) and R. Scott Kemp (MIT) improved this manuscript. PL and PH were partially supported by the Harvard Global Institute. MS was partially supported by the National Institute Of General Medical Sciences of the National Institutes of Health under Award Number R01GM130668. The content is solely the responsibility of the authors and does not necessarily represent the official views of the National Institutes of Health.

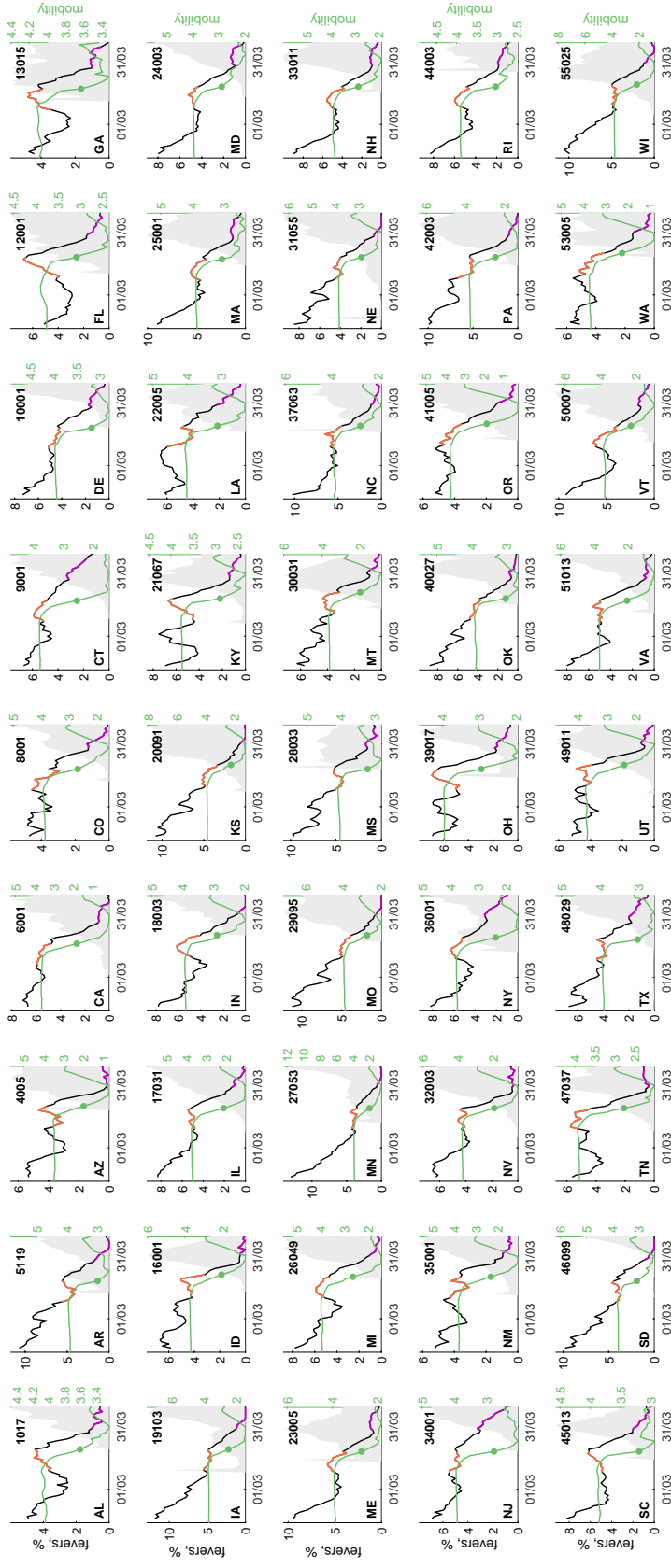


Figure 1: Variations in mobility, fever incidence, and confirmed COVID-19 cases for an example county in each of 45 U.S. states. Each panel shows a mobility index (green), the estimated percentage of individuals experiencing fevers (black), and new daily COVID-19 cases (gray shading). The midpoint of mobility reductions (green dot) is used to define an early fever interval, corresponding to F_1 , over the preceding 10 days (red line), and a later fever interval, F_2 , between 10 to 20 days afterwards (purple line). COVID-19 cases are normalized such that their maximum value aligns with the upper limit of the y-axis, and the mobility index is centered such that its maximum value equals the average fever incidence during F_1 . Both COVID-19 cases and mobility are smoothed using a seven-day moving average. Panel labels indicate two-letter state abbreviations and county FIPS code (see Table S1). Omitted states have no county with more than 100 confirmed COVID-19 cases as of April 10, 2020.

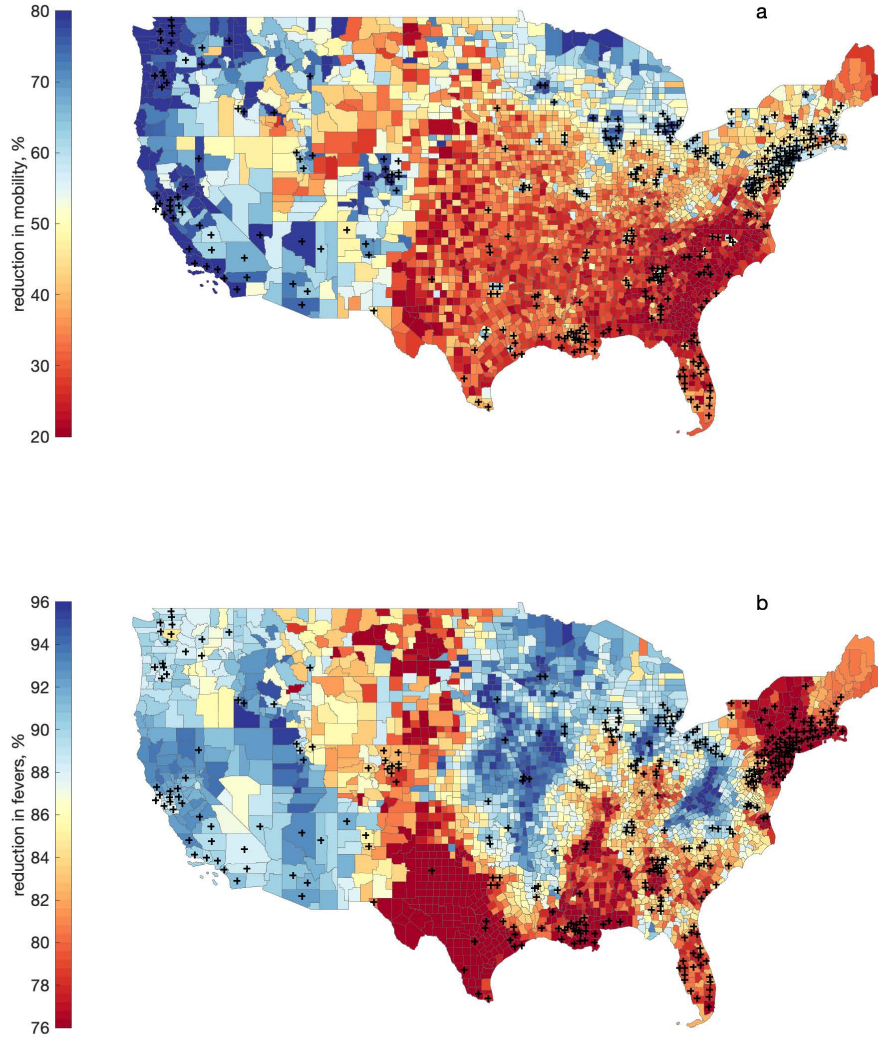


Figure 2: Average reductions in mobility and fevers for U.S. counties. **(a)** Fractional reductions in mobility, δM , are computed as the range in mobility divided by maximum mobility between March 5th and April 15th, $\delta M = (M_{\max} - M_{\min})/M_{\max}$ **(b)** Fractional reduction in fever, δF , computed as the change in fevers across the drop in mobility divided by fevers prior to the drop in mobility, $\delta F = (F_1 - F_2)/F_1$ (see Figure 1). Counties having more than 100 confirmed COVID-19 cases as of April 10, 2020 (indicated by cross marks) are included in regression analyses shown in Figure 3.

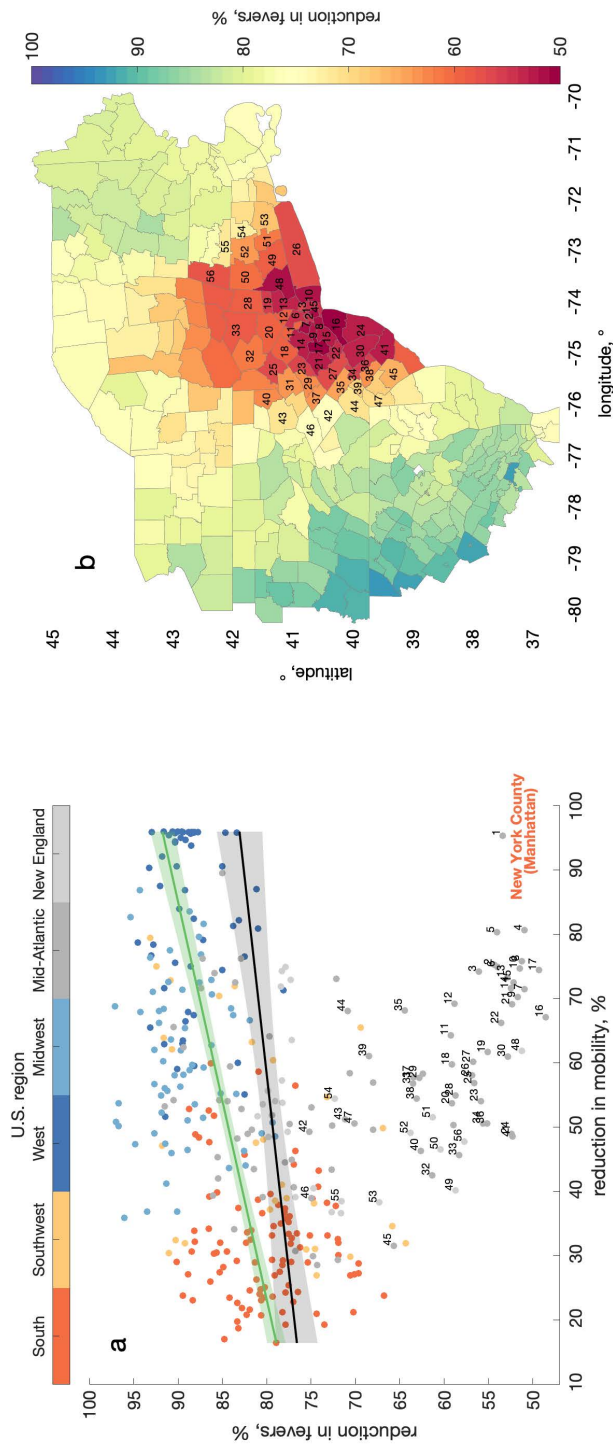


Figure 3: Relationship between reductions in mobility and fever across the 368 U.S. counties having more than 100 confirmed COVID-19 cases. **(a)** Regression of reductions in fevers, δF , against reductions in mobility, δM , gives a slope of $0.81 \pm 0.28\%$ reduction in fevers per 10% reduction in mobility (black line and shading). Excluding New York City and counties within 500 km leads to a steeper regression relationship of $1.6 \pm 0.13\%$ reduction in fevers per 10% reduction in mobility (green line and shading). **(b)** Fractional reduction in fevers, δF , in counties within 500 km of New York City. Numbering is provided for counties within 200 km of New York City and corresponds to that in panel (a).

References

- [1] Brownstein, J. S., Freifeld, C. C., Reis, B. Y., and Mandl, K. D. (2008). Surveillance Sans Frontieres: Internet-based emerging infectious disease intelligence and the HealthMap project. *PLoS Medicine*, 5(7).
- [2] Butler, D. (2013). When Google got flu wrong: US outbreak foxes a leading web-based method for tracking seasonal flu. *Nature*, 494(7436):155–157.
- [3] Center for Disease Control and Prevention (2020). Weekly U.S. Influenza Surveillance Report.
- [4] Chamberlain, S. D., Singh, I., Ariza, C. A., Daitch, A. L., Philips, P. B., and Dalziel, B. D. (2020). Real-time detection of covid-19 epicenters within the united states using a network of smart thermometers. *medRxiv*.
- [5] Chinazzi, M., Davis, J. T., Ajelli, M., Gioannini, C., Litvinova, M., Merler, S., y Piontti, A. P., Mu, K., Rossi, L., Sun, K., et al. (2020). The effect of travel restrictions on the spread of the 2019 novel coronavirus (COVID-19) outbreak. *Science*.
- [6] Cook, S., Conrad, C., Fowlkes, A. L., and Mohebbi, M. H. (2011). Assessing google flu trends performance in the united states during the 2009 influenza virus a (h1n1) pandemic. *PloS one*, 6(8).
- [7] Dalziel, B. D., Kissler, S., Gog, J. R., Viboud, C., Bjørnstad, O. N., Metcalf, C. J. E., and Grenfell, B. T. (2018). Urbanization and humidity shape the intensity of influenza epidemics in US cities. *Science*, 362(6410):75–79.
- [8] Drake, J. M. (2005). Limits to forecasting precision for outbreaks of directly transmitted diseases. *PLoS Med*, 3(1):e3.
- [9] Frost, C. and Thompson, S. G. (2000). Correcting for regression dilution bias: comparison

- of methods for a single predictor variable. *Journal of the Royal Statistical Society: Series A (Statistics in Society)*, 163(2):173–189.
- [10] Generous, N., Fairchild, G., Deshpande, A., Del Valle, S. Y., and Priedhorsky, R. (2014). Global disease monitoring and forecasting with Wikipedia. *PLoS Computational Biology*, 10(11).
- [11] Gershman, J. (2020). A Guide to State Coronavirus Lockdowns. *The Wall Street Journal*.
- [12] Ginsberg, J., Mohebbi, M. H., Patel, R. S., Brammer, L., Smolinski, M. S., and Brilliant, L. (2009). Detecting influenza epidemics using search engine query data. *Nature*, 457(7232):1012–1014.
- [13] Hsiang, S., Allen, D., Annan-Phan, S., Bell, K., Bolliger, I., Chong, T., Druckenmiller, H., Hultgren, A., Huang, L. Y., Krasovich, E., et al. (2020). The Effect of Large-Scale Anti-Contagion Policies on the Coronavirus (COVID-19) Pandemic. *medRxiv*.
- [14] J. David Goodman (2020). How Delays and Unheeded Warnings Hindered New Yorks Virus Fight.
- [15] Kaashoek, J. and Santillana, M. (2020). COVID-19 positive cases, evidence on the time evolution of the epidemic or an indicator of local testing capabilities? A case study in the United States. *arXiv*.
- [16] Kissler, S. M., Tedijanto, C., Goldstein, E., Grad, Y. H., and Lipsitch, M. (2020). Projecting the transmission dynamics of sars-cov-2 through the postpandemic period. *Science*.
- [17] Kraemer, M. U., Yang, C.-H., Gutierrez, B., Wu, C.-H., Klein, B., Pigott, D. M., du Plessis, L., Faria, N. R., Li, R., Hanage, W. P., et al. (2020a). The effect of human mobility and control measures on the COVID-19 epidemic in China. *Science*.
- [18] Kraemer, M. U., Yang, C.-H., Gutierrez, B., Wu, C.-H., Klein, B., Pigott, D. M., du Plessis, L., Faria, N. R., Li, R., Hanage, W. P., et al. (2020b). The effect of human mobility and control measures on the COVID-19 epidemic in China. *Science*.

- [19] Kucharski, A. J., Russell, T. W., Diamond, C., Liu, Y., Edmunds, J., Funk, S., Eggo, R. M., Sun, F., Jit, M., Munday, J. D., et al. (2020). Early dynamics of transmission and control of COVID-19: a mathematical modelling study. *The Lancet Infectious Diseases*.
- [20] Lai, S., Ruktanonchai, N. W., Zhou, L., Prosper, O., Luo, W., Floyd, J. R., Wesolowski, A., Santillana, M., Zhang, C., Du, X., Yu, H., et al. (2020). Effect of non-pharmaceutical interventions for containing the COVID-19 outbreak: an observational and modelling study. *medRxiv*.
- [21] Lauer, S. A., Grantz, K. H., Bi, Q., Jones, F. K., Zheng, Q., Meredith, H. R., Azman, A. S., Reich, N. G., and Lessler, J. (2020). The incubation period of coronavirus disease 2019 (COVID-19) from publicly reported confirmed cases: estimation and application. *Annals of Internal Medicine*.
- [22] Lazer, D., Kennedy, R., King, G., and Vespignani, A. (2014). The parable of google flu: traps in big data analysis. *Science*, 343(6176):1203–1205.
- [23] Li, Q., Guan, X., Wu, P., Wang, X., Zhou, L., Tong, Y., Ren, R., Leung, K. S., Lau, E. H., Wong, J. Y., et al. (2020). Early transmission dynamics in Wuhan, China, of novel coronavirus-infected pneumonia. *New England Journal of Medicine*.
- [24] Lipsitch, M. and Santillana, M. (2019). Enhancing situational awareness to prevent infectious disease outbreaks from becoming catastrophic. *Global Catastrophic Biological Risks*, pages 59–74.
- [25] Liu, Y., Gayle, A. A., Wilder-Smith, A., and Rocklöv, J. (2020). The reproductive number of COVID-19 is higher compared to SARS coronavirus. *Journal of Travel Medicine*.
- [26] Ma, J. (2020). Estimating Epidemic Exponential Growth Rate And Basic Reproduction Number. *Infectious Disease Modelling*.
- [27] Miller, A. C., Singh, I., Koehler, E., and Polgreen, P. M. (2018). A smartphone-driven

- thermometer application for real-time population-and individual-level influenza surveillance. *Clinical Infectious Diseases*, 67(3):388–397.
- [28] Moriyama, M., Hugentobler, W. J., and Iwasaki, A. (2020). Seasonality of respiratory viral infections. *Annual Review of Virology*, 7.
- [29] National Academies of Sciences, E. and Medicine (2020). *Rapid Expert Consultation on SARS-CoV-2 Survival in Relation to Temperature and Humidity and Potential for Seasonality for the COVID-19 Pandemic (April 7, 2020)*. The National Academies Press, Washington, DC.
- [30] Nishiura, H., Kobayashi, T., Miyama, T., Suzuki, A., Jung, S., Hayashi, K., Kinoshita, R., Yang, Y., Yuan, B., Akhmetzhanov, A. R., et al. (2020). Estimation of the asymptomatic ratio of novel coronavirus infections (COVID-19). *medRxiv*.
- [31] Nsoesie, E. O., Butler, P., Ramakrishnan, N., Mekar, S. R., and Brownstein, J. S. (2015). Monitoring disease trends using hospital traffic data from high resolution satellite imagery: a feasibility study. *Scientific Reports*, 5:9112.
- [32] OAG Aviation Worldwide (2020). Coronavirus and the impact on airline schedules. <https://www.oag.com/coronavirus-airline-schedules-data>. Accessed: 2020-04-20.
- [33] Paolotti, D., Carnahan, A., Colizza, V., Eames, K., Edmunds, J., Gomes, G., Koppeschaar, C., Rehn, M., Smallegange, R., Turbelin, C., et al. (2014). Web-based participatory surveillance of infectious diseases: the InfluenzaNet participatory surveillance experience. *Clinical Microbiology and Infection*, 20(1):17–21.
- [34] Paul, M. J., Dredze, M., and Broniatowski, D. (2014). Twitter improves influenza forecasting. *PLoS Currents*, 6.
- [35] Pepe, E., Bajardi, P., Gauvin, L., Privitera, F., Lake, B., Cattuto, C., and Tizzoni, M. (2020). COVID-19 outbreak response: a first assessment of mobility changes in Italy following national lockdown. *medRxiv*.

- [36] Radin, J. M., Wineinger, N. E., Topol, E. J., and Steinhubl, S. R. (2020). Harnessing wearable device data to improve state-level real-time surveillance of influenza-like illness in the USA: a population-based study. *The Lancet Digital Health*.
- [37] Salathe, M., Bengtsson, L., Bodnar, T. J., Brewer, D. D., Brownstein, J. S., Buckee, C., Campbell, E. M., Cattuto, C., Khandelwal, S., Mabry, P. L., et al. (2012). Digital epidemiology. *PLoS Computational Biology*, 8(7).
- [38] Santillana, M., Nguyen, A., Louie, T., Zink, A., Gray, J., Sung, I., and Brownstein, J. S. (2016). Cloud-based electronic health records for real-time, region-specific influenza surveillance. *Scientific Reports*, 6:25732.
- [39] Santillana, M., Nsoesie, E. O., Mearu, S. R., Scales, D., and Brownstein, J. S. (2014a). Using clinicians search query data to monitor influenza epidemics. *Clinical Infectious Diseases*, 59(10):1446.
- [40] Santillana, M., Zhang, D. W., Althouse, B. M., and Ayers, J. W. (2014b). What can digital disease detection learn from (an external revision to) google flu trends? *American Journal of Preventive Medicine*, 47(3):341–347.
- [41] Seattle Children’s Hospital (2020). Infection Exposure Table. <https://www.seattlechildrens.org/conditions/a-z/infection-exposure-questions/>. Accessed: 2020-04-20.
- [42] Smolinski, M. S., Crawley, A. W., Baltrusaitis, K., Chunara, R., Olsen, J. M., Wójcik, O., Santillana, M., Nguyen, A., and Brownstein, J. S. (2015). Flu near you: crowdsourced symptom reporting spanning 2 influenza seasons. *American Journal of Public Health*, 105(10):2124–2130.
- [43] Stock, J. H. (2020). Coronavirus data gaps and the policy response to the novel coronavirus.
- [44] The New York Times (2020). Coronavirus Map: Tracking the Global Outbreak. <https://www.nytimes.com/interactive/2020/world/coronavirus-maps.html>.

- [45] U.S. Census Bureau (2020). County population totals: 2010-2019. <https://www.census.gov/data/datasets/time-series/demo/popest/2010s-counties-total.html>. Accessed: 2020-04-20.
- [46] U.S. Centers for Disease Control (2020). COVID-19 Travel Recommendations by Country.
- [47] Viboud, C., Charu, V., Olson, D., Ballesteros, S., Gog, J., Khan, F., Grenfell, B., and Simonsen, L. (2014). Demonstrating the use of high-volume electronic medical claims data to monitor local and regional influenza activity in the US. *PloS One*, 9(7).
- [48] Wallinga, J. and Lipsitch, M. (2007). How generation intervals shape the relationship between growth rates and reproductive numbers. *Proceedings of the Royal Society B: Biological Sciences*, 274(1609):599–604.
- [49] Watts, D. J., Muhamad, R., Medina, D. C., and Dodds, P. S. (2005). Multiscale, resurgent epidemics in a hierarchical metapopulation model. *Proceedings of the National Academy of Sciences*, 102(32):11157–11162.
- [50] Wu, F., Zhao, S., Yu, B., Chen, Y.-M., Wang, W., Song, Z.-G., Hu, Y., Tao, Z.-W., Tian, J.-H., Pei, Y.-Y., et al. (2020). A new coronavirus associated with human respiratory disease in China. *Nature*, 579(7798):265–269.
- [51] Yang, S., Santillana, M., and Kou, S. C. (2015). Accurate estimation of influenza epidemics using Google search data via ARGO. *Proceedings of the National Academy of Sciences*, 112(47):14473–14478.
- [52] Yang, Y., Yang, M., Shen, C., Wang, F., Yuan, J., Li, J., Zhang, M., Wang, Z., Xing, L., Wei, J., et al. (2020). Laboratory diagnosis and monitoring the viral shedding of 2019-ncov infections. *MedRxiv*.
- [53] Zhou, F., Yu, T., Du, R., Fan, G., Liu, Y., Liu, Z., Xiang, J., Wang, Y., Song, B., Gu, X., et al. (2020). Clinical course and risk factors for mortality of adult inpatients with COVID-19 in Wuhan, China: a retrospective cohort study. *The Lancet*.

Supplemental Material for

Fever and mobility data indicate social distancing has reduced incidence of communicable disease in the United States

Parker Liautaud*, Peter Huybers, and Mauricio Santillana

*Corresponding author, e-mail: parker.liautaud@g.harvard.edu

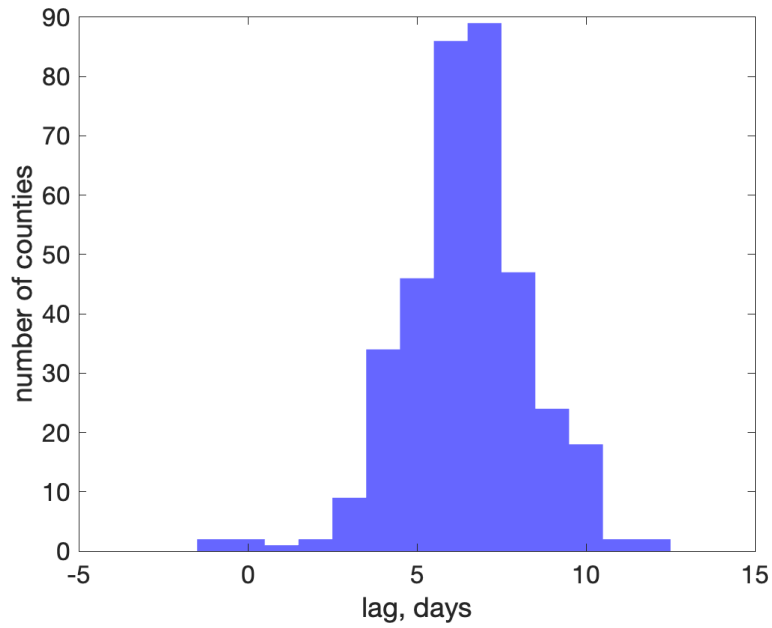


Figure S1: Lag of the change in fever incidences, F , behind a change in mobility, M , for 368 U.S. counties having at least 100 confirmed cases of COVID-19 as of April 10, 2020, where the lag is estimated using data for F and M between March 5 and April 15. The mean lag is 6.5 days with 95% of counties giving lags between 3 and 10 days.

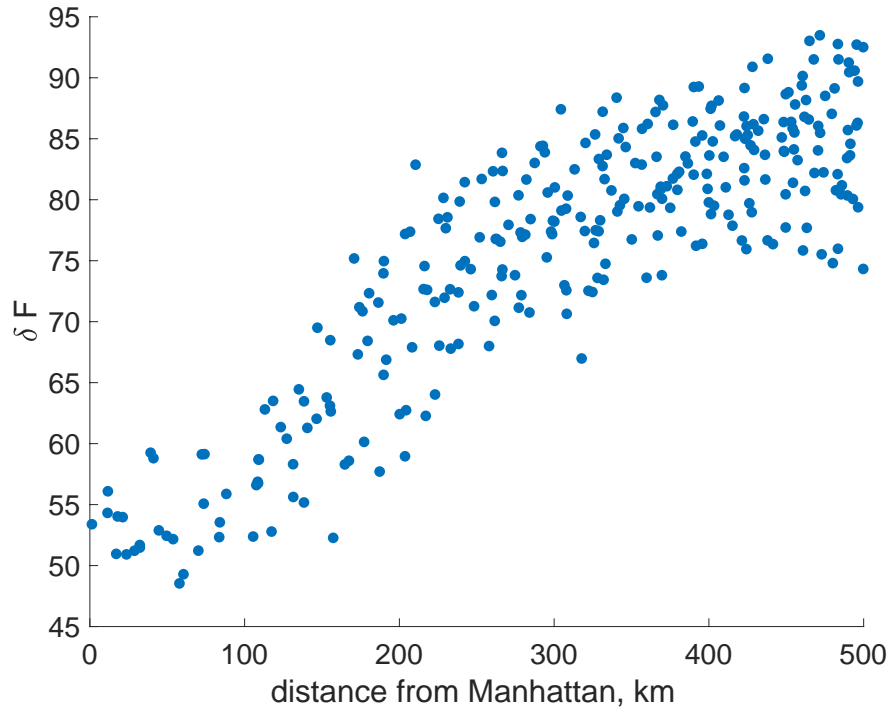


Figure S2: Reduction in fever incidences, δF , for 299 counties that are centered less than 500 km from Manhattan in New York City. Within this region, a county's distance from New York City is strongly correlated with the extent to which its fevers are reduced over a thirty day period ($r = 0.87$, $p < 0.01$).

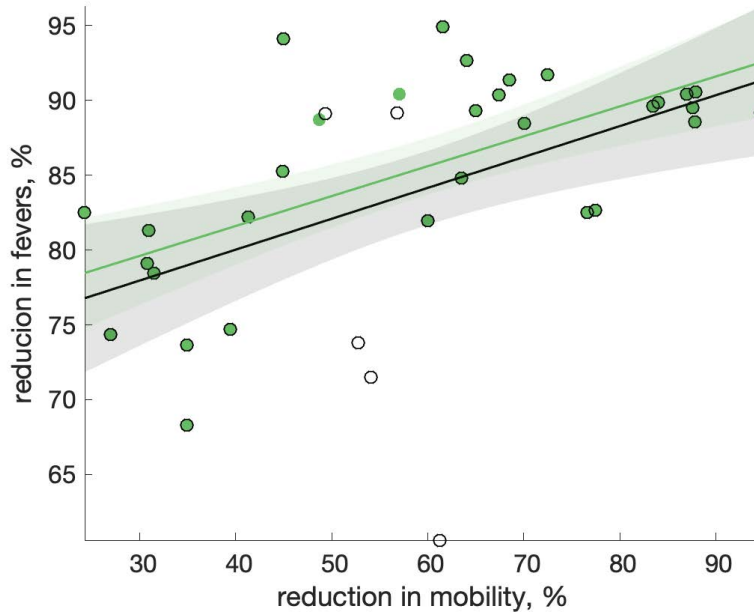


Figure S3: Relationship between reduction in fevers and reduction in mobility after spatially averaging counties having more than 100 confirmed COVID-19 cases into 5° latitude by 5° longitude bins. The regression indicates a $2.1 \pm 0.6\%$ reduction in fevers for every 10% reduction in mobility (black markers, line, and shading). If excluding counties within 500 km of New York City, the regression slope is $2.0 \pm 0.4\%$ reduction in fevers for every 10% reduction in mobility (green markers, line, and shading) and the r^2 increases from 0.27 to 0.42.

Table S1: Fractional changes in mobility and subsequent changes in fever incidences for the 368 counties shown in Figure 3 of the main text. Counties are ranked from greatest to least reduction in mobility, and are identified by their Federal Information Processing Standard (FIPS) code.

Rank	County	State	FIPS	$\delta M, \%$	$\delta F, \%$
1	Orange County	CA	6059	96.0	90.6
2	Ventura County	CA	6111	96.0	89.6
3	Placer County	CA	6061	96.0	91.6
4	Los Angeles County	CA	6037	96.0	90.1
5	Contra Costa County	CA	6013	96.0	89.5
6	Snohomish County	WA	53061	95.9	88.3
7	Santa Clara County	CA	6085	95.9	87.8
8	Kitsap County	WA	53035	95.9	88.5
9	San Mateo County	CA	6081	95.9	88.1
10	Sonoma County	CA	6097	95.9	92.9
11	Washington County	OR	41067	95.9	88.3
12	Marin County	CA	6041	95.9	88.8
13	Alameda County	CA	6001	95.9	88.4
14	Boulder County	CO	8013	95.9	83.4
15	Multnomah County	OR	41051	95.8	88.5
16	Whatcom County	WA	53073	95.8	88.2
17	King County	WA	53033	95.8	84.7
18	Island County	WA	53029	95.7	90.3
19	San Francisco County	CA	6075	95.7	88.6
20	San Diego County	CA	6073	95.4	91.0
21	New York County	NY	36061	95.4	53.4
22	Skagit County	WA	53057	95.0	89.7
23	Spokane County	WA	53063	94.7	89.2
24	Clark County	WA	53011	94.5	90.3
25	Santa Barbara County	CA	6083	94.3	90.3
26	Clackamas County	OR	41005	93.8	88.5
27	Sacramento County	CA	6067	92.1	91.8
28	Denver County	CO	8031	90.6	85.0
29	Pierce County	WA	53053	90.6	90.1
30	San Luis Obispo County	CA	6079	90.4	93.3
31	Arlington County	VA	51013	89.5	85.0
32	Solano County	CA	6095	87.6	92.0
33	Douglas County	CO	8035	87.1	81.1
34	Blaine County	ID	16013	86.9	89.2
35	Hennepin County	MN	27053	86.9	94.3
36	Clark County	NV	32003	84.0	89.9

Rank	County	State	FIPS	$\delta M, \%$	$\delta F, \%$
37	Washtenaw County	MI	26161	83.6	88.7
38	Ramsey County	MN	27123	82.7	95.4
39	Marion County	OR	41047	82.4	88.2
40	Jefferson County	CO	8059	82.2	83.1
41	Oakland County	MI	26125	81.6	87.1
42	Eagle County	CO	8037	81.3	83.8
43	Arapahoe County	CO	8005	80.9	81.0
44	Kings County	NY	36047	80.7	51.0
45	Queens County	NY	36081	80.4	54.0
46	DuPage County	IL	17043	79.6	87.6
47	Coconino County	AZ	4005	79.5	93.2
48	Benton County	WA	53005	79.1	87.2
49	Ada County	ID	16001	78.7	94.5
50	Washoe County	NV	32031	78.4	92.8
51	Dane County	WI	55025	77.6	90.9
52	Lake County	IL	17097	76.9	87.4
53	Fresno County	CA	6019	76.7	93.0
54	Larimer County	CO	8069	76.6	82.5
55	Ingham County	MI	26065	76.4	93.2
56	Montgomery County	MD	24031	76.3	87.2
57	Fairfax County	VA	51059	76.2	82.9
58	Richmond County	NY	36085	75.9	51.2
59	Gallatin County	MT	30031	75.6	90.3
60	Hudson County	NJ	34017	75.3	54.3
61	Pima County	AZ	4019	75.1	92.4
62	Riverside County	CA	6065	75.0	88.6
63	Chittenden County	VT	50007	75.0	77.9
64	Bergen County	NJ	34003	75.0	54.0
65	Nassau County	NY	36059	74.7	51.5
66	Summit County	UT	49043	74.5	85.0
67	Somerset County	NJ	34035	74.5	49.3
68	Suffolk County	MA	25025	74.3	78.3
69	Bronx County	NY	36005	74.2	56.1
70	Alexandria County	VA	51510	74.0	85.9
71	Westchester County	NY	36119	73.4	52.9
72	Tompkins County	NY	36109	73.1	72.2
73	Norfolk County	MA	25021	73.0	77.3
74	Kane County	IL	17089	73.0	86.3
75	Maricopa County	AZ	4013	72.9	90.8
76	Milwaukee County	WI	55079	72.6	91.1
77	Cook County	IL	17031	72.6	87.6
78	Loudoun County	VA	51107	72.6	83.5
79	Middlesex County	NJ	34023	72.5	52.2
80	Bernalillo County	NM	35001	72.0	83.6

Rank	County	State	FIPS	$\delta M, \%$	$\delta F, \%$
81	Middlesex County	MA	25017	71.9	78.4
82	San Joaquin County	CA	6077	71.6	91.5
83	Howard County	MD	24027	71.6	87.4
84	Morris County	NJ	34027	71.6	52.4
85	Essex County	NJ	34013	71.5	50.9
86	Waukesha County	WI	55133	71.4	89.5
87	El Paso County	CO	8041	71.3	78.1
88	Macomb County	MI	26099	71.1	92.8
89	McHenry County	IL	17111	70.7	86.2
90	Sandoval County	NM	35043	70.4	85.4
91	Union County	NJ	34039	70.3	51.7
92	Rockland County	NY	36087	69.2	58.8
93	Hunterdon County	NJ	34019	69.2	52.3
94	Johnson County	KS	20091	68.8	97.1
95	St. Louis County	MO	29510	68.5	84.0
96	Livingston County	MI	26093	68.4	91.6
97	Montgomery County	PA	42091	68.2	64.5
98	Wayne County	MI	26163	68.1	92.1
99	Chester County	PA	42029	68.1	70.9
100	Grant County	WA	53025	68.0	88.9
101	Olmsted County	MN	27109	67.9	94.2
102	St. Louis County	MO	29189	67.4	83.8
103	San Bernardino County	CA	6071	67.4	88.2
104	Monmouth County	NJ	34025	67.2	48.5
105	Will County	IL	17197	66.7	81.9
106	Salt Lake County	UT	49035	66.5	89.2
107	Mercer County	NJ	34021	66.2	53.5
108	Hamilton County	IN	18057	66.2	92.1
109	Allegheny County	PA	42003	65.6	90.5
110	Utah County	UT	49049	65.5	93.1
111	Travis County	TX	48453	65.5	69.4
112	Kent County	MI	26081	65.4	89.2
113	Passaic County	NJ	34031	64.3	59.3
114	Monroe County	NY	36055	64.1	79.7
115	Pinal County	AZ	4021	63.9	91.6
116	Genesee County	MI	26049	63.7	90.8
117	Hampshire County	MA	25015	63.6	77.2
118	Davis County	UT	49011	63.5	89.4
119	Collin County	TX	48085	63.2	81.7
120	Kern County	CA	6029	63.0	89.5
121	Stanislaus County	CA	6099	62.9	91.5
122	St. Charles County	MO	29183	62.8	86.2
123	Butler County	PA	42019	62.4	89.4
124	Navajo County	AZ	4017	62.1	90.7

Rank	County	State	FIPS	$\delta M, \%$	$\delta F, \%$
125	Johnson County	IA	19103	62.1	92.7
126	Cuyahoga County	OH	39035	62.0	89.7
127	Fairfield County	CT	9001	61.9	51.2
128	Putnam County	NY	36079	61.7	55.1
129	Delaware County	PA	42045	61.1	68.5
130	Burlington County	NJ	34005	61.0	52.8
131	Denton County	TX	48121	60.5	79.3
132	Lorain County	OH	39093	60.3	91.7
133	Bucks County	PA	42017	60.2	56.7
134	Adams County	CO	8001	60.1	83.3
135	Williamson County	TN	47187	59.9	86.3
136	Sussex County	NJ	34037	59.8	59.1
137	Franklin County	OH	39049	59.7	88.4
138	Yakima County	WA	53077	59.5	88.2
139	Erie County	NY	36029	59.5	84.1
140	Kenosha County	WI	55059	59.3	87.1
141	Tulare County	CA	6107	59.1	90.1
142	Lake County	OH	39085	58.9	88.7
143	Fulton County	GA	13121	58.6	80.9
144	Onondaga County	NY	36067	58.5	70.6
145	Albany County	NY	36001	58.4	62.4
146	Summit County	OH	39153	58.2	89.4
147	Saginaw County	MI	26145	58.1	90.4
148	Suffolk County	NY	36103	58.1	56.9
149	Lehigh County	PA	42077	57.7	63.5
150	Northampton County	PA	42095	57.7	62.8
151	Essex County	MA	25009	57.3	78.3
152	Saratoga County	NY	36091	56.9	68.0
153	Pike County	PA	42103	56.9	56.6
154	Monroe County	PA	42089	56.8	63.5
155	Lucas County	OH	39095	56.7	92.7
156	Orleans County	LA	22071	56.5	76.8
157	Portage County	OH	39133	56.3	89.8
158	St. Clair County	MI	26147	56.1	91.5
159	Monroe County	MI	26115	55.7	91.2
160	Worcester County	MA	25027	55.6	79.9
161	St. Clair County	IL	17163	55.3	85.2
162	Hamilton County	OH	39061	55.2	83.5
163	Weld County	CO	8123	55.2	82.5
164	Jackson County	MI	26075	55.0	91.9
165	Dutchess County	NY	36027	55.0	58.7
166	Fort Bend County	TX	48157	54.7	73.2
167	Tolland County	CT	9013	54.5	72.3
168	Gloucester County	NJ	34015	54.4	63.1

Rank	County	State	FIPS	$\delta M, \%$	$\delta F, \%$
169	Frederick County	MD	24021	54.2	85.4
170	Beaver County	PA	42007	54.2	90.5
171	Carroll County	MD	24013	54.1	84.4
172	Warren County	NJ	34041	54.1	55.9
173	Rockingham County	NH	33015	54.0	79.0
174	Plymouth County	MA	25023	53.8	78.2
175	Orange County	NY	36071	53.7	59.1
176	Polk County	IA	19153	53.7	96.7
177	Cumberland County	ME	23005	53.6	80.4
178	Lake County	IN	18089	53.6	88.1
179	Westmoreland County	PA	42129	53.2	91.5
180	Dauphin County	PA	42043	53.1	75.0
181	Durham County	NC	37063	52.9	88.8
182	Lancaster County	PA	42071	52.8	82.9
183	Wake County	NC	37183	52.6	86.5
184	Mahoning County	OH	39099	52.3	91.8
185	Niagara County	NY	36063	51.9	79.4
186	Forsyth County	GA	13117	51.8	86.0
187	Hillsborough County	NH	33011	51.8	81.0
188	Canyon County	ID	16027	51.7	91.4
189	Middlesex County	CT	9007	51.6	61.3
190	Hendricks County	IN	18063	51.5	87.2
191	Luzerne County	PA	42079	51.2	71.2
192	St. Joseph County	IN	18141	51.1	88.9
193	Jackson County	MO	29095	50.8	97.0
194	Butler County	OH	39017	50.7	79.4
195	New Castle County	DE	10003	50.6	70.1
196	Camden County	NJ	34007	50.6	55.2
197	Philadelphia County	PA	42101	50.6	55.6
198	Anne Arundel County	MD	24003	50.5	77.4
199	Cape May County	NJ	34009	50.4	59.0
200	Broome County	NY	36007	50.3	72.6
201	Allen County	IN	18003	50.2	96.7
202	Williamson County	TX	48491	49.9	66.9
203	York County	PA	42133	49.6	81.7
204	Schenectady County	NY	36093	49.6	68.0
205	Franklin County	MA	25011	49.3	77.7
206	Berks County	PA	42011	49.3	75.2
207	Hartford County	CT	9003	49.1	63.8
208	Kankakee County	IL	17091	49.1	80.6
209	Linn County	IA	19113	49.1	92.7
210	Ocean County	NJ	34029	49.0	52.4
211	Prince William County	VA	51153	49.0	82.1
212	Davidson County	TN	47037	48.9	88.0

Rank	County	State	FIPS	$\delta M, \%$	$\delta F, \%$
213	Decatur County	IN	18031	48.6	79.0
214	Atlantic County	NJ	34001	48.6	52.3
215	York County	ME	23031	48.5	79.8
216	Mecklenburg County	NC	37119	48.4	87.6
217	Prince George's County	MD	24033	48.3	83.3
218	El Paso County	TX	48141	48.1	80.4
219	Berkshire County	MA	25003	47.8	57.7
220	DeKalb County	GA	13089	47.7	86.5
221	Brazos County	TX	48041	47.6	81.2
222	Marion County	IN	18097	47.5	91.4
223	Douglas County	NE	31055	47.4	94.8
224	San Juan County	NM	35045	47.2	91.8
225	Litchfield County	CT	9005	46.6	60.4
226	Stark County	OH	39151	46.5	88.9
227	St. James County	LA	22093	46.4	76.8
228	Lackawanna County	PA	42069	46.4	62.6
229	Montgomery County	OH	39113	46.3	82.5
230	Trumbull County	OH	39155	46.0	90.8
231	Cobb County	GA	13067	45.8	82.5
232	Ulster County	NY	36111	45.7	58.3
233	James City County	VA	51095	45.4	85.5
234	Oneida County	NY	36065	45.0	77.2
235	Baltimore County	MD	24005	44.6	77.9
236	East Baton Rouge County	LA	22033	44.2	76.9
237	Miami County	OH	39109	44.0	82.4
238	Johnson County	IN	18081	43.6	84.3
239	Harford County	MD	24025	43.5	81.4
240	Lebanon County	PA	42075	43.4	72.7
241	Ascension County	LA	22005	43.3	74.1
242	Sullivan County	NY	36105	42.6	61.4
243	Richmond County	VA	51760	42.0	85.5
244	Madison County	IN	18095	41.3	91.3
245	Dallas County	TX	48113	41.1	78.3
246	Shelby County	TN	47157	40.7	74.2
247	Baltimore County	MD	24510	40.6	77.0
248	Barnstable County	MA	25001	40.6	74.7
249	New Haven County	CT	9009	40.2	58.7
250	Sumner County	TN	47165	39.9	85.6
251	Alachua County	FL	12001	39.7	79.6
252	Henrico County	VA	51087	39.4	86.1
253	Madison County	AL	1089	39.2	86.5
254	Bristol County	MA	25005	39.2	76.8
255	Charles County	MD	24017	39.2	80.5
256	Cameron County	TX	48061	39.0	77.8

Rank	County	State	FIPS	$\delta M, \%$	$\delta F, \%$
257	Schuylkill County	PA	42107	39.0	75.0
258	St. Tammany County	LA	22103	38.9	74.8
259	Fayette County	KY	21067	38.8	81.0
260	Montgomery County	TX	48339	38.6	79.1
261	Hampden County	MA	25013	38.5	71.6
262	New London County	CT	9011	38.3	67.3
263	Shelby County	AL	1117	38.3	73.2
264	Hidalgo County	TX	48215	38.1	74.7
265	Iberville County	LA	22047	38.0	78.7
266	Jefferson County	AL	1073	37.8	72.2
267	Jefferson County	KY	21111	37.5	83.2
268	Collier County	FL	12021	37.3	77.9
269	Tarrant County	TX	48439	37.2	79.6
270	Sedgwick County	KS	20173	36.9	90.1
271	Minnehaha County	SD	46099	36.9	93.5
272	Palm Beach County	FL	12099	36.8	78.0
273	Providence County	RI	44007	36.8	72.7
274	Kent County	RI	44003	36.7	71.6
275	Lee County	FL	12071	36.7	80.5
276	Orange County	FL	12095	36.1	77.4
277	Wyandotte County	KS	20209	35.9	96.1
278	Broward County	FL	12011	35.8	77.9
279	Osceola County	FL	12097	35.3	77.5
280	Lafayette County	LA	22055	35.1	78.4
281	Washington County	LA	22117	34.6	79.2
282	Bexar County	TX	48029	34.6	65.8
283	Gwinnett County	GA	13135	34.2	86.6
284	Chesterfield County	VA	51041	34.2	83.6
285	St. Martin County	LA	22099	34.0	81.8
286	Pulaski County	AR	5119	33.9	88.2
287	Wilson County	TN	47189	33.7	82.2
288	Tangipahoa County	LA	22105	33.5	76.6
289	Seminole County	FL	12117	33.5	77.5
290	Plaquemines County	LA	22075	33.2	73.1
291	Miami-Dade County	FL	12086	33.2	75.1
292	Sarasota County	FL	12115	33.2	79.4
293	St. Johns County	FL	12109	32.8	77.2
294	St. Charles County	LA	22089	32.6	72.0
295	Cherokee County	GA	13057	32.6	81.8
296	Tulsa County	OK	40143	32.5	90.3
297	Forsyth County	NC	37067	32.2	88.1
298	Lafourche County	LA	22057	32.1	71.9
299	Bossier County	LA	22015	32.1	85.2
300	Martin County	FL	12085	32.0	82.3

Rank	County	State	FIPS	$\delta M, \%$	$\delta F, \%$
301	Webb County	TX	48479	32.0	64.3
302	Cleveland County	OK	40027	32.0	89.2
303	Hinds County	MS	28049	31.9	77.3
304	Cumberland County	NJ	34011	31.6	65.6
305	DeSoto County	MS	28033	31.3	76.3
306	Harris County	TX	48201	31.1	74.6
307	Galveston County	TX	48167	31.0	75.6
308	Sussex County	DE	10005	30.8	76.8
309	Caddo County	LA	22017	30.7	88.4
310	Charleston County	SC	45019	30.7	84.5
311	Early County	GA	13099	30.5	85.6
312	Oklahoma County	OK	40109	30.5	91.0
313	Rutherford County	TN	47149	30.4	85.9
314	St. John the Baptist County	LA	22095	30.1	71.9
315	Virginia Beach County	VA	51810	30.0	74.8
316	Brazoria County	TX	48039	29.8	70.6
317	Manatee County	FL	12081	29.4	79.4
318	Livingston County	LA	22063	29.4	72.0
319	Kent County	DE	10001	29.4	72.0
320	Pinellas County	FL	12103	29.3	78.2
321	De Soto County	LA	22031	29.2	83.4
322	Lake County	FL	12069	29.1	77.2
323	Guilford County	NC	37081	29.0	90.2
324	Henry County	GA	13151	29.0	81.3
325	Rapides County	LA	22079	29.0	75.3
326	Jefferson County	LA	22051	28.8	69.7
327	Hillsborough County	FL	12057	28.6	78.3
328	Chesapeake County	VA	51550	28.6	74.3
329	Lee County	GA	13177	28.2	84.9
330	Pasco County	FL	12101	27.5	78.5
331	Dougherty County	GA	13095	27.4	85.3
332	St. Bernard County	LA	22087	27.3	69.6
333	Terrebonne County	LA	22109	27.1	70.1
334	Ouachita County	LA	22073	27.1	88.9
335	Iberia County	LA	22045	27.0	70.6
336	Lubbock County	TX	48303	27.0	74.4
337	Brevard County	FL	12009	26.9	79.1
338	Houston County	GA	13153	26.3	81.1
339	Mitchell County	GA	13205	26.0	86.3
340	Calcasieu County	LA	22019	25.4	77.5
341	Lee County	AL	1081	25.1	80.2
342	Polk County	FL	12105	24.8	80.7
343	Volusia County	FL	12127	24.6	81.9
344	Carroll County	GA	13045	24.4	76.5

Rank	County	State	FIPS	$\delta M, \%$	$\delta F, \%$
345	Beaufort County	SC	45013	24.3	77.9
346	York County	SC	45091	24.1	80.8
347	Knox County	TN	47093	23.9	89.5
348	Jackson County	MS	28059	23.8	66.8
349	Chatham County	GA	13051	23.7	79.3
350	St. Lucie County	FL	12111	23.5	80.3
351	Richland County	SC	45079	23.5	84.2
352	Hall County	GA	13139	23.1	88.3
353	Clayton County	GA	13063	23.1	80.6
354	Douglas County	GA	13097	22.9	77.0
355	Greenville County	SC	45045	22.7	83.3
356	Duval County	FL	12031	21.9	82.8
357	Horry County	SC	45051	21.6	81.9
358	Mobile County	AL	1097	21.3	70.3
359	Clay County	FL	12019	21.3	78.2
360	Muscogee County	GA	13215	21.0	74.4
361	Chambers County	AL	1017	20.9	82.3
362	Sumter County	GA	13261	20.8	80.6
363	Lexington County	SC	45063	19.8	83.3
364	Escambia County	FL	12033	19.3	73.5
365	Bartow County	GA	13015	19.3	77.9
366	Kershaw County	SC	45055	18.8	83.2
367	Spartanburg County	SC	45083	17.0	84.8
368	Sumter County	SC	45085	16.5	79.0